Journal of the American College of Cardiology
© 2005 by the American College of Cardiology Foundation
Published by Elsevier Inc.

Vol. 45, No. 6, 2005
ISSN 0735-1097/05/$30.00
doi:10.1016/j.jacc.2004.12.026

Atherosclerosis

Does Shear Stress Modulate Both Plaque Progression and Regression in the Thoracic Aorta?

Human Study Using Serial Magnetic Resonance Imaging

Jolanda J. Wentzel, PHD,*‖ Roberto Corti, MD,*‡ Zahi A. Fayad, PHD,† Paul Wisdom, BSC,† Frank Macaluso, BSC,† Mark O. Winkelman, MSC,§ Valentin Fuster, MD, PHD,§ Juan J. Badimon, PHD‡

New York, New York; Nijkerk and Rotterdam, the Netherlands

OBJECTIVES The purpose of this study was to investigate the role of shear stress (SS) in plaque regression.

BACKGROUND A condition favorable to the development of atherosclerotic lesions is low oscillating SS. In the descending thoracic aorta, the relationship between plaque distribution and SS has never been characterized. The regression of plaque as the result of lipid-lowering therapy is associated with reverse atherogenic mechanisms. Therefore, we investigated the role of SS in plaque regression. Magnetic resonance imaging (MRI) provides a unique opportunity to noninvasively study morphology and hemodynamics.

METHODS Cross-sectional images of atherosclerotic plaques in the descending thoracic aorta of 10 asymptomatic, hypercholesteremic patients were acquired at baseline and 24 months after starting lipid-lowering therapy by using a black-blood sequence on a 1.5-T clinical MRI system (5 mm $\times$ 780 μm $\times$ 780 μm). Average wall thickness (WT) was derived per quadrant. The aorta was subdivided in segments 2 cm in length starting 1 cm from the aortic arch.

RESULTS Average WT decreased with increasing distance from the arch (3.0 $\pm$ 0.7 mm vs. 2.5 $\pm$ 0.3 mm; $p < 0.05$) and showed a helical pattern from the proximal to distal segments. Phase-contrast MRI was performed in the thoracic aorta of eight healthy volunteers to derive typical average SS distribution. Shear stress predicted the location of WT ($r^2 = 0.29$, $p < 0.05$) but did not predict plaque regression. The best predictor of plaque regression was baseline WT.

CONCLUSIONS Our data showing an association between WT and average low SS locations support the role of local hemodynamics in the development of atherosclerotic lesions in descending thoracic aorta. Furthermore, SS does not seem to be the major predictor for plaque regression by lipid-lowering interventions. Therefore, our data suggest that other mechanisms are involved in the lipid-reversal mechanism. (J Am Coll Cardiol 2005;45:846–54) © 2005 by the American College of Cardiology Foundation

Atherosclerotic plaques are not distributed equally in the vascular system (1,2). They are more prevalent, for instance, in the inner curve of coronary arteries (2,3), closer to side branches (4), in the aortic arch, and in the bulb of the carotid arteries (5). These are sites of flow separation (6) and oscillating shear stress (SS) (4), suggesting that SS plays a role in the distribution of plaques in the vascular system (3).

From the *Cardiovascular Institute, †Imaging Science Laboratory, and ‡Cardiovascular Biology Research Laboratory, Mount Sinai School of Medicine, New York, New York; §Damen Dredging Equipment, Research Department, Nijkerk, the Netherlands; and the ‖Thoraxcenter, Erasmus Medical Center, Rotterdam, the Netherlands. This study was supported by grants from NIH-SCOR HL54469 (to Drs. Fuster and Badimon), NHLBI-HL61801 (to Dr. Fuster), the New York Community Trust (to Dr. Fayad), the Dutch Atherosclerosis Society (to Dr. Wentzel), the Haak-Bastiaanse-Kuneman Stichting (to Dr. Wentzel), the Swiss National Research Foundation (to Dr. Corti), and Merck and Co. Dr. Fayad received research grants from National Institutes of Health/National Heart, Lung, and Blood Institute, GlaxoSmithKline, Cordis (J&J), and Schering AG. Dr. Badimon received a research grant from Merck and is on the advisory boards of AstraZeneca and BMS. Mark O. Winkelman is an employee of Damen Dredging Equipment, Research Department, Nijkerk, the Netherlands.

Manuscript received August 6, 2004; revised manuscript received November 12, 2004, accepted December 14, 2004.

Velocity measurements of the blood flow in the thoracic aorta (7,8) have suggested a very distinct pattern in SS, including low and high SS regions, because of the extraordinary curvature of the aortic arch preceding the thoracic aorta. The study of atherosclerotic plaques in the descending thoracic aorta mainly is performed using transesophageal echocardiography. Until now, no studies have described the relationship between the location of atherosclerotic plaques and SS in the descending thoracic aorta.

Plaque regression after long-term hypolipidemic treatment with statins (9) has been related to depletion of lipid content from the plaques (10). Recent studies have suggested that statins may act by interfering with several mechanisms involved in atherogenesis: they reverse endothelial dysfunction, reduce the hyperaggregability of platelets, reduce inflammation, and improve reverse cholesterol transport, leading to lesion stabilization. Nonlipid-dependent effects (called pleiotropic) been have also postulated. The question is whether SS also modulates the plaque regression that is attributed to lipid-lowering therapy.

Abbreviations and Acronyms

ANOVA = analysis of variance
LDL = low-density lipoprotein
MRI = magnetic resonance imaging
NWT = normalized wall thickness
SS = shear stress
WT = wall thickness
$WT_{baseline}$ = wall thickness at baseline

Magnetic resonance imaging (MRI) is a unique technique that allows for the study of flow, blood velocity profiles, and vessel wall morphology. This technique has been used to characterize the dependency of lesions to hemodynamics in the abdominal aorta (4,11). In this study, we applied high-resolution serial MRI, aiming to study the relationship between plaque development and plaque regression that is attributed to lipid-lowering therapy in asymptomatic hypercholesteremic patients with the characteristic SS patterns of healthy volunteers in the descending thoracic aorta.

METHODS

Study population and experimental design. Asymptomatic hypercholesterolemic patients showing atherosclerotic plaques in the thoracic aorta were selected randomly from a cohort of patients who were included in a regression study using statins to lower lipid levels (9,12). Patients were included based on the pre-existence of atherosclerotic plaques (>2 mm) in the thoracic aorta detected by B-mode ultrasound transesophageal echocardiography or MRI. Data of the thoracic descending aorta of 10 patients (5 men, 58 ± 8 years; 5 women, 66 ± 7 years, 15 atherosclerotic lesions) were acquired at baseline and at 24 months after starting simvastatin therapy by using MRI. Magnetic resonance imaging was performed on a 1.5-T whole-body MRI system (Signa CV/I; GEMS; 40 mT/m; SR150), and the protocol was performed as described previously (9).

In nine healthy volunteers (three women, six men, 31 ± 7 years) who were not aware of having any atherosclerotic disease, phase-contrast MRI was applied with the following settings: 1.5-T Siemens, slice thickness 5 mm, field of view 21 × 28 cm, 192 × 256 pixels, a velocity encoding of 250 cm/s through plane velocity (13), and breath hold. The velocity measurements were taken at each 2 cm starting from the arch.

To ensure correct rotational registration of the MR images at baseline versus follow-up, the line joining sternal to the vertebral body was used as a reference. The Mount Sinai School of Medicine medical ethical committee approved the study, and every person gave informed consent to participate.

Morphometric data. The MR images showing plaques, with a minimal extension of 2 cm, were transferred to a computer and carefully matched for the two different time points using several anatomical landmarks. To derive high-resolution local wall thicknesses (WT) from the MR cross sections of the descending thoracic aorta, the contours were obtained with a custom-made software program that facilitated the manual tracing of the lumen and wall contours. The contours were compared with the contours obtained previously (12) and were not used to reanalyze the original data set. The WT was derived as distance from the lumen contour to the outer wall contour, along the line passing through the luminal center of mass (14). Each cross section was divided into four quadrants. The quadrants (i to iv) were determined by a frontal and sagittal planes crossing at the center of mass (Fig. 1A). The average WT of each quadrant at baseline and 24 months follow-up was calculated, and the circumferential location and axial location (as distance from the reference cross section at the aortic arch, Fig. 1B) were documented. Subsequently, the cross sections were subdivided into four segments (Fig. 1B)

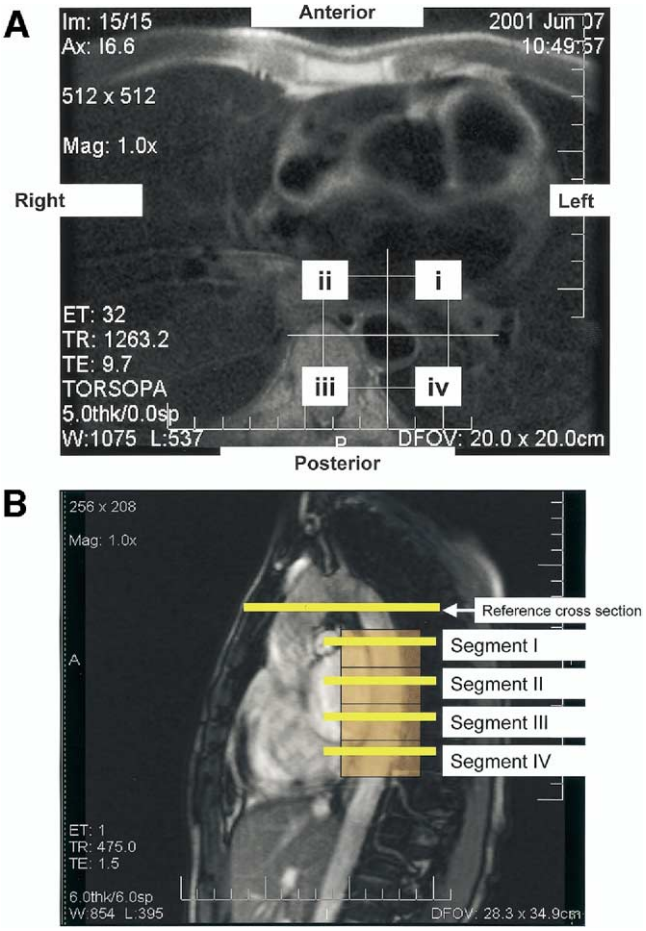

Figure 1. **(A)** Location of the predefined quadrants i, ii, iii, and iv relative to the right, left, anterior, and posterior side of the patient. **(B)** Axial distribution of the four predefined segments **(orange)**, each 2 cm in length, summarizing the wall thickness data beginning 1 cm from the reference cross section, located at the exit of the aortic arch. Segment I is located 1 to 3 cm from reference cross section; segment II is located 3 to 5 cm from reference cross section; segment III is located 5 to 7 cm from reference cross section; and segment IV is located 7 to 9 cm from reference cross section. The location of phase-contrast velocity measurements, in **yellow**, is positioned in the center of the defined segments. Magnetic resonance imaging slice thickness for the velocity and wall velocity measurements was 5 mm.

containing four consecutive cross sections (slice thickness, 0.5 mm) covering 2 cm in length each, starting 1 cm distal from the arch. Per quadrant, the average WT in each segment was calculated resulting in a maximum of 16 data points per patient (four quadrants × four segments). The same approach was followed for the 24 months of follow-up data.

Shear stress determination. Because the velocity measurements were taken at each 2 cm starting from the arch, they were located in the center of the segments defined by the average WT (Fig. 1B). For each cross section at each time point, first, a moving average filter (3 × 3) was applied to the obtained through plane velocity profile, thereby reducing noise (an example of this result is shown in Fig. 2A). The two-dimensional derivative of the velocity field, derived from the shear rate in x and y direction (Fig. 2B), defined the local shear rates in the lumen of the vessel (Fig. 2C). The shear rate at the wall was determined by the maximum of the absolute shear rate in the 16 closest regions to the vessel wall. The 16 areas were determined by the outer 10% of the vessel radius and 22.5° in a circumferential direction determined from the center of mass (Figs. 2D and 2E). Averaging the cardiac cycle and the quadrants, as defined previously (Fig. 1A), the time averaged shear rate per quadrant was delivered. Shear rate times viscosity (3 cPoise) determined the SS (3,15).

Statistics. The average WT per segment and quadrant was obtained from the averages per location per patient. The differences in WT and SS per quadrant and segment were compared by applying two-way analysis of variance (ANOVA). Normalization of the WT per patient was performed relative to the average WT per segment per patient so that existing asymmetric patterns in WT distribution are emphasized independent of the absolute thickness.

The average WT at baseline for all patients at 16 locations (four segments × four quadrants) was related to the time-averaged SS at the same 16 locations by regression analysis. Similar regression analysis was applied to the normalized baseline WT (NWT) and SS. The best predictor of plaque regression during a 24-month period of treatment, which was WT at baseline ($WT_{baseline}$) or SS, was investigated using stepwise regression analysis. A value of $p < 0.05$ was considered significant. SPSS 11.0 (SPSS Institute, Chicago, Illinois) was used for all the statistical analysis.

RESULTS

Wall thickness. At baseline, atherosclerotic thickening of the descending thoracic aorta was observed in 93 cross

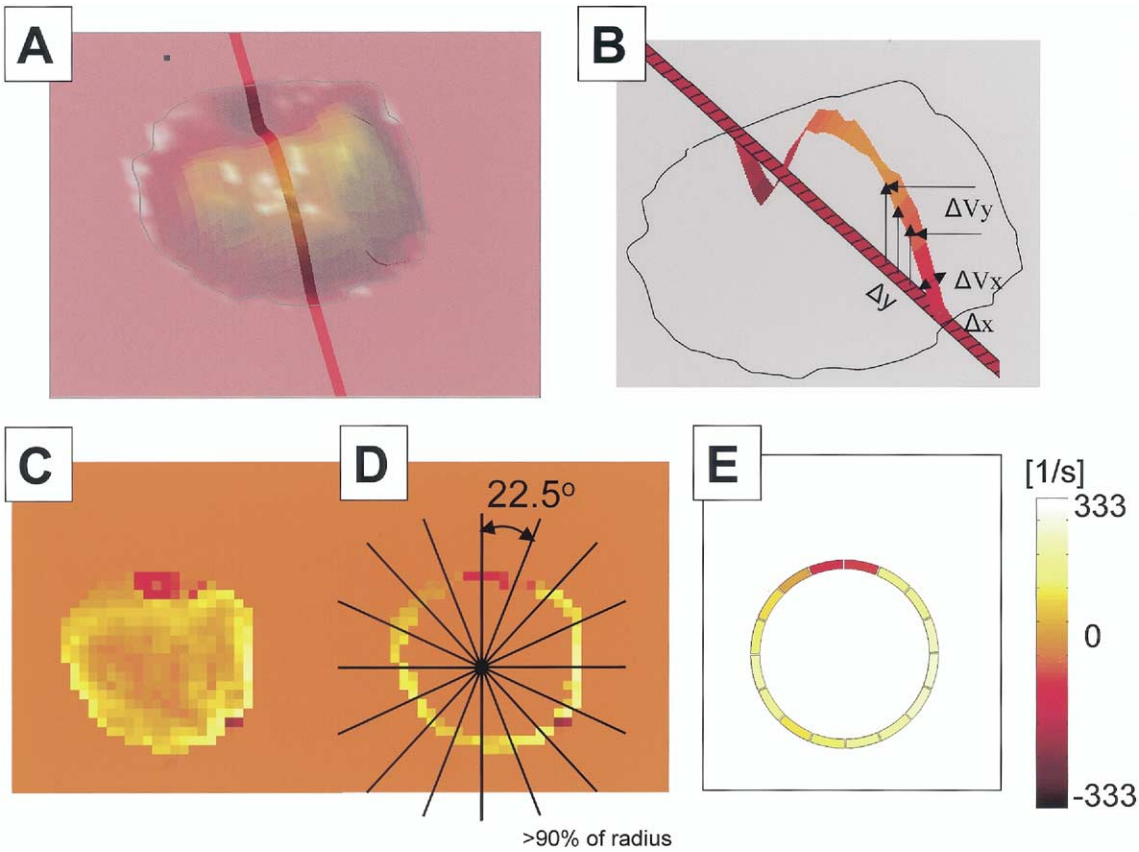

Figure 2. Shear rate determination from velocity profile. **(A)** The velocity profile measured at segment I at one moment during the cardiac cycle after smoothing is applied. **(B)** Visualization of determination of velocity gradient (dv/dr). **(C)** Shear rate at each pixel in the lumen. **(D)** Determination of shear rate at the vessel wall, with the maximum shear rate in regions of approximately 22.5° at the outer 10% of the radius. **(E)** Shear rate at 16 locations along the circumference; these are summarized into four quadrants per cross section.

Table 1. Total Number of Cross Sections per Patient per Segment Showing Atherosclerosis at Baseline and Included in the Study for Average Wall Thickness Calculations

	Segment			
Patient	**I**	**II**	**III**	**IV**
1	3	4	4	
2		2	3	
3	2	4	4	2
4	4	4	4	4
5	2	3		
6		4	3	2
7		2	4	2
8	2	4	4	
9	4	4		
10	3	4		2

sections in 10 patients. Per patient, the distribution of lesions over the predefined segments is presented in Table 1. The average WT was 2.8 ± 0.5 mm (range 1.9 to 4.6 mm). The average WT was maximal at segment I and decreased linearly when traveling distally to segment IV (3.0 ± 0.7 mm; 2.8 ± 0.5 mm; 2.7 ± 0.4 mm; and 2.5 ± 0.3 mm for segments I to IV, respectively). The average WT at segment I (3.0 ± 0.7 mm) was statistically different from segment IV (2.5 ± 0.3 mm, $p < 0.05$).

Subdividing the segments into quadrants revealed that atherosclerotic WT was asymmetric and was preferentially located at the left side (quadrant i and quadrant iv) of the patients (Figs. 3E to 3H). The average $WT_{baseline}$ for the 16 predefined quadrants distributed over the four segments was statistically different (two-way ANOVA, $p < 0.05$). The average plaque distribution resembled the distribution in the individual patient shown in Figures 3I to 3L.

Normalization of the WT per segment underlines the asymmetry in plaque distribution regardless of the absolute WT values (Table 2). The helical pattern in NWT distribution can be appreciated in Figures 3M to 3P; the quadrants in which the average WT is greater or equal to the average at each segment are highlighted in orange (also see Table 2).

Effect of statin treatment. At the systemic level, statin therapy maintained during a period of 24 months resulted in a significant reduction of 23% and 35% in total cholesterol

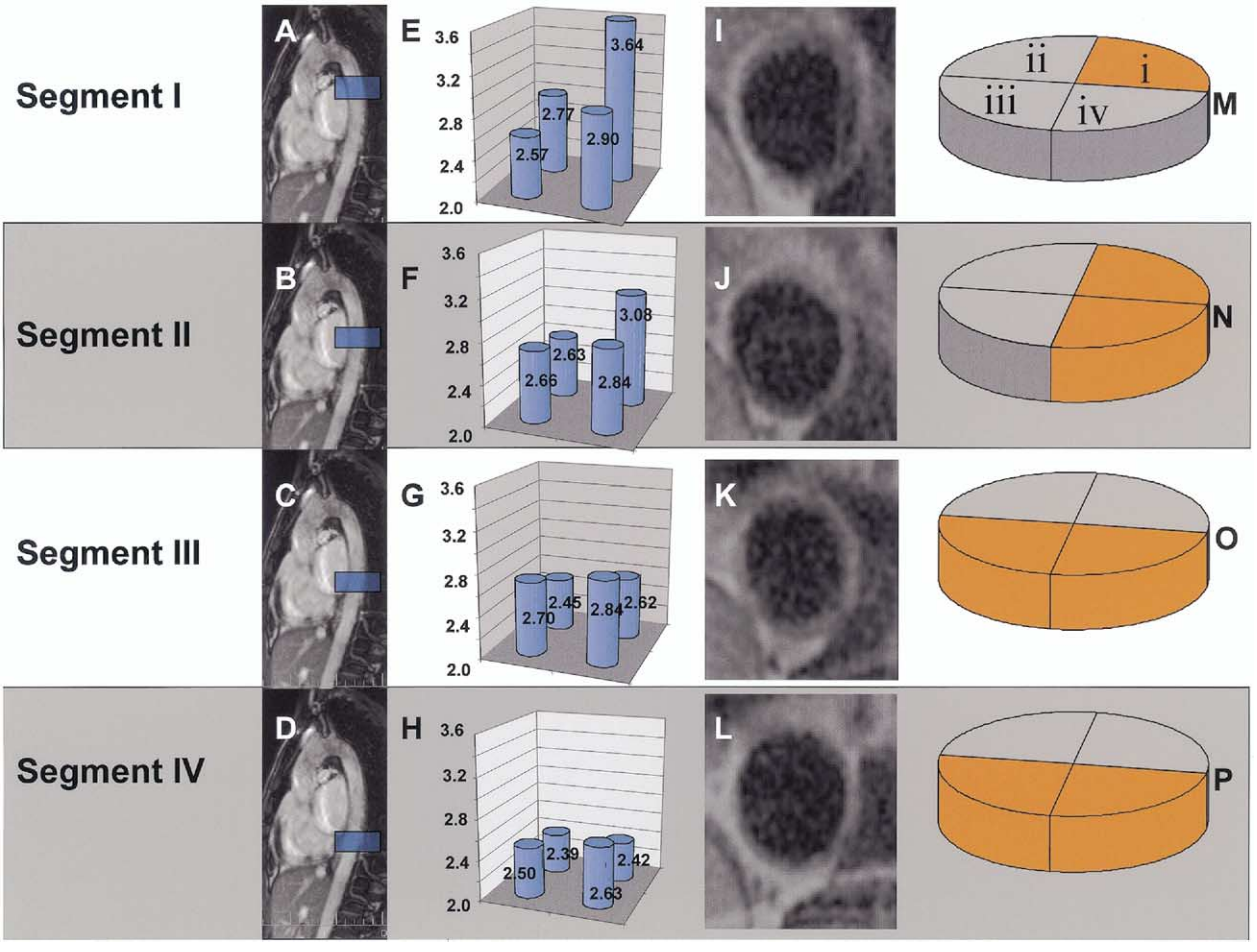

Figure 3. Plaque distribution depending on axial and circumferential location **(A to D)** location of segments I to IV on magnetic resonance imaging overview of aorta. **(E to H)** Average wall thickness at baseline for quadrants i to iv for segments I to IV. **(I to L)** Magnetic resonance imaging cross sections of aorta of individual patient at segments I to IV. **(M to P)** Quadrants with an average relative wall thickness exceeding the average of the segment are shown in **orange**.

Table 2. Average Normalized Wall Thickness at Baseline per Segment and Quadrant

Segment	Quadrant			
	i	ii	iii	iv
I	1.23 ± 0.15	0.94 ± 0.16	0.87 ± 0.11	0.96 ± 0.15
II	1.09 ± 0.13	0.94 ± 0.11	0.95 ± 0.11	1.02 ± 0.12
III	0.99 ± 0.09	0.93 ± 0.10	1.01 ± 0.08	1.07 ± 0.15
IV	0.97 ± 0.11	0.96 ± 0.10	1.00 ± 0.11	1.06 ± 0.17

and low-density lipoprotein (LDL) fraction, respectively, whereas high-density lipoprotein cholesterol levels increased slightly. At the vascular level, statin therapy was associated with a reduction in atherosclerotic plaques as described previously (9,12). Because of the much smaller number of plaques studied in this article, the observed plaque regression did not reach statistically significance: −0.055 mm, $p = 0.2$. Examining this in greater detail, we found that plaque regression was dependent on the distance from the aortic arch (Fig. 4) and observed predominantly at the proximal segments (I, II, and III), with an average of −0.06 mm ($n = 12$, $p < 0.05$). In addition, plaque regression after 24 months of statin treatment was directly related to the $WT_{baseline}$ ($WT_{follow\text{-}up} - WT_{baseline} = 0.6 - 0.23 \times WT_{baseline}$ [mm], $p < 0.05$, $r^2 = 0.26$; Fig. 4, $n = 16$, (four quadrants and four segments).

Shear stress. Because of technical reasons, the data of one healthy volunteer could not be used for further analysis. Therefore, only eight data sets, containing 128 quadrants, are included in this study. The average SS over the cardiac cycle was 0.36 N/m^2 ± 0.17 N/m^2, ranging from −0.05 N/m^2 to 0.79 N/m^2 ($n = 128$). The average SS per segment is visualized in Figure 5, which shows no gradient in longitudinal direction over the segments (p = NS). However, subdivision of the segments into quadrants revealed an asymmetrical distribution of the low SS areas (two-way ANOVA, $p < 0.05$). Greater analysis of the most proximal segment (segment I) showed that, in all the eight volunteers, the average SS was at a minimum for quadrant i (quadrant i vs. quadrants ii, iii, and iv: 0.17 ± 0.12 N/m^2, $n = 8$, vs. 0.42 ± 0.15 N/m^2, $n = 24$, *t* test, $p < 0.05$, Fig. 5) and at a maximum at quadrant iii (quadrant iii vs. quadrants i, ii, and iv: 0.49 ± 0.15 N/m^2, $n = 8$, vs. 0.32 ± 0.17 N/m^2, $n = 24$, *t* test, $p < 0.05$).

Relationship between WT and SS. Atherosclerotic wall thickening in the patients followed a similar pattern as the low SS in the healthy volunteers, resulting in an inverse relationship between $WT_{baseline}$ and SS ($WT_{baseline} = -1.6 \times SS + 3.3$ [mm], $r^2 = 0.29$, $p < 0.05$, Fig. 6A). Therefore, the classical pathology observations of atherosclerotic plaque location are confirmed in vivo by noninvasive MRI. Normalization of the $WT_{baseline}$ measurements (NWT) showed that for each axial segment, the variations in $WT_{baseline}$ could be explained by the variations in SS ($NWT = -0.63 \times SS + 1.23$, $r^2 = 0.59$, $p < 0.05$, Fig. 6B).

Predictor of plaque regression. No relationship was observed between plaque regression attributed to 24 months of statin treatment and SS. Multivariate stepwise analysis that included SS and $WT_{baseline}$ as predictors showed that $WT_{baseline}$ was the strongest predictor for plaque regression after 24 months of statin treatment ($p < 0.05$)

DISCUSSION

We have investigated the relationship between SS and the development and regression of atherosclerotic plaques. Our data indicate that the presence of atherosclerotic plaques in the descending thoracic aorta is associated with the local average low SS locations, which suggests there is a role for low SS condition in the development of atherosclerotic lesions. To investigate the potential effect of SS on plaque regression, after baseline imaging of the established atherosclerotic lesions, we instituted statin therapy in all patients during a period of two years. Overall, the lipid-lowering intervention resulted in a marked hypolipidemic effect, leading to a significant reduction of plaque volume (9,12). Plaque regression in the subgroup of patients selected for this study was not related to local SS patterns but was fully explained by local WT at baseline. Although it is known from several studies that the prevalence of atherosclerotic plaques in the thoracic aorta is very low (6.3%) (16), many studies support the relationship between thoracic aorta atherosclerotic disease and the risk of subsequent vascular events, including coronary artery disease (17,18) and stroke (19).

Wall thickness. The maximal $WT_{baseline}$ of the atherosclerotic plaques in this study was similar to the observations of Shunk et al. (20) but a bit smaller than described by Fayad et al. (3.6 mm vs. 4.6 mm) (21) and Cohen et al. (22). The difference might be explained by the patient population that was studied. In this study, only asymptomatic patients were investigated and, thus, were expected to be in an early stage of atherosclerosis, whereas the other studies included patients experiencing transient ischemic attacks or stroke.

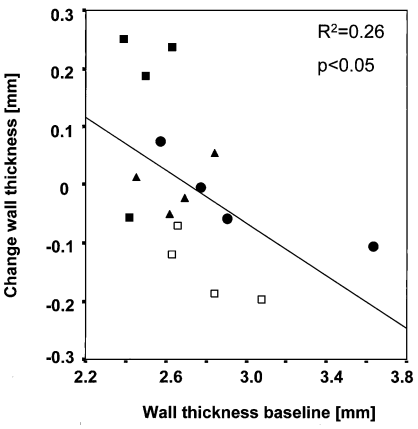

Figure 4. Relationship between change in wall thickness (wall $thickness_{follow\text{-}up}$ − wall $thickness_{baseline}$) attributable to 24 months of treatment with simvastatin and wall thickness at baseline. **Closed circles** = 1 to 3 cm, segment I; **open squares** = 3 to 5 cm, segment II; **closed triangles** = 5 to 7 cm, segment III; **closed squares** = 7 to 9 cm, segment IV.

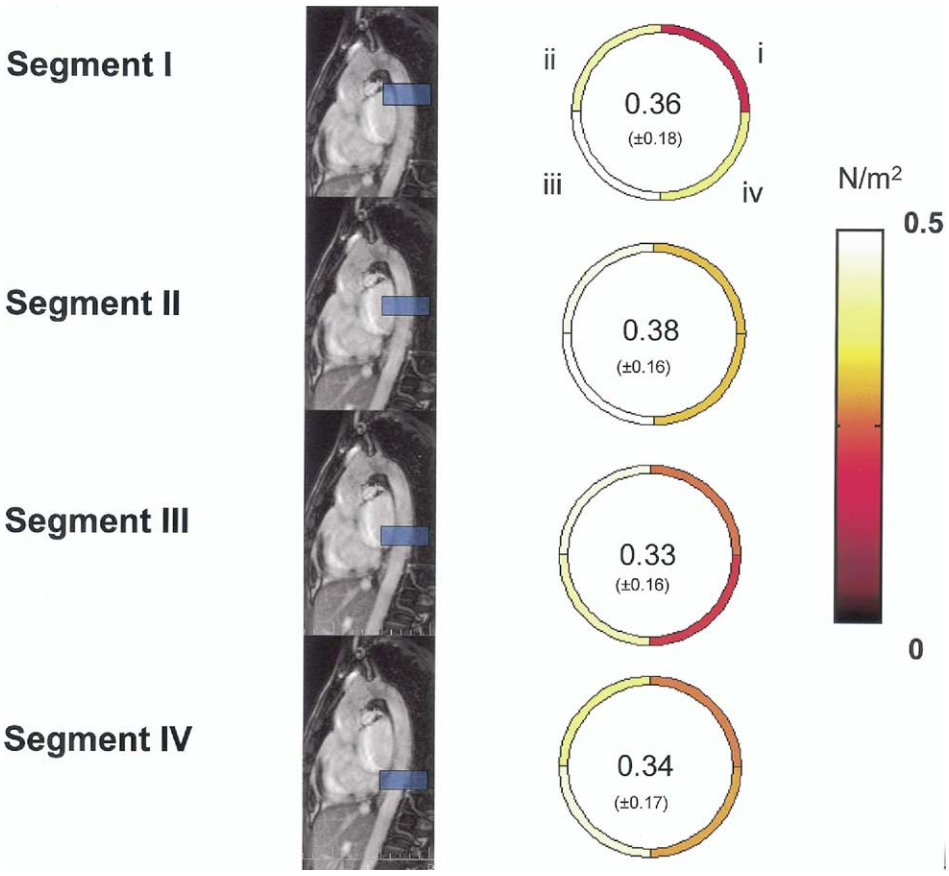

Figure 5. Shear stress distribution depending on axial and circumferential location with average shear stress for segment in **center of circle** (standard deviation). **Color coding** refers to average shear stress over cardiac cycle per quadrant.

Until now only limited data have been available describing plaque localization in the descending thoracic aorta. A tendency of predisposition to atherogenesis in the posterior thoracic aorta has been suggested previously (23). In addition, histology data from the left side of the thoracic aorta obtained from young adolescents, that is, The Pathobiological Determinants of Atherosclerosis in Youth (PDAY) data, showed that in the proximal segment, not only the posterior but also the anterior side is affected with atherosclerotic plaques (24). Similarly, we found in the most proximal segment atherosclerotic WT mainly in the left anterior side, whereas for the more distal segments, this thickness occurred at the left posterior side (Fig. 3). The reason for reduced data availability about plaque distribution in the thoracic aorta might be related to the difficulty in studying this arterial location in vivo. Transesophageal echocardiography is used as standard technique; however, it does not allow visualization of the entire thoracic aorta (i.e., 360°), a deficiency that is attributed to near-field signal losses. Interestingly, the few cross-sectional images reported in literature demonstrate the atherosclerotic plaques at the same left side of the patient (17,21).

Shear stress. Time-averaged SS was derived from velocity measurements in the thoracic aorta of healthy young volunteers to assess the characteristic natural SS distribution. Although individual variations are reported in the literature, amidst the normal subjects, a helical velocity distribution was observed regardless the age of the volunteers (25,26). Indeed, the peak velocity might decrease with increasing age, but this will be of minor influence on the relative SS distribution (25). Moreover, the presence of helical flow was not associated with the patient's age (8). Because the presence of the helix usually is studied, there is not much information available on the SS distribution in the thoracic aorta of healthy or diseased subjects.

Because SS is determined by multiplying viscosity and local shear rates, which is the radial derivative of the velocity, its value is sensitive for noise. Several techniques have been adopted to reduce noise in the SS determination from phase-contrast MRI (27,28). In this study, SS was determined applying a smoothing filter in combination with a radial derivative. The accuracy of the methods used to obtain SS from the phase-contrast velocity profiles was tested with a numerically derived parabolic profile generated with similar resolution (1 mm $\times$ 1 mm) and average peak velocity (150 cm/s) and vessel diameter (2 cm) as the MRI data. An underestimation of 9.6 $\pm$ 1.5% in SS values was found for this particular example, which is comparable with previous studies (27,28). It is not likely that the obtained spatial gradients in SS distribution measured as average over

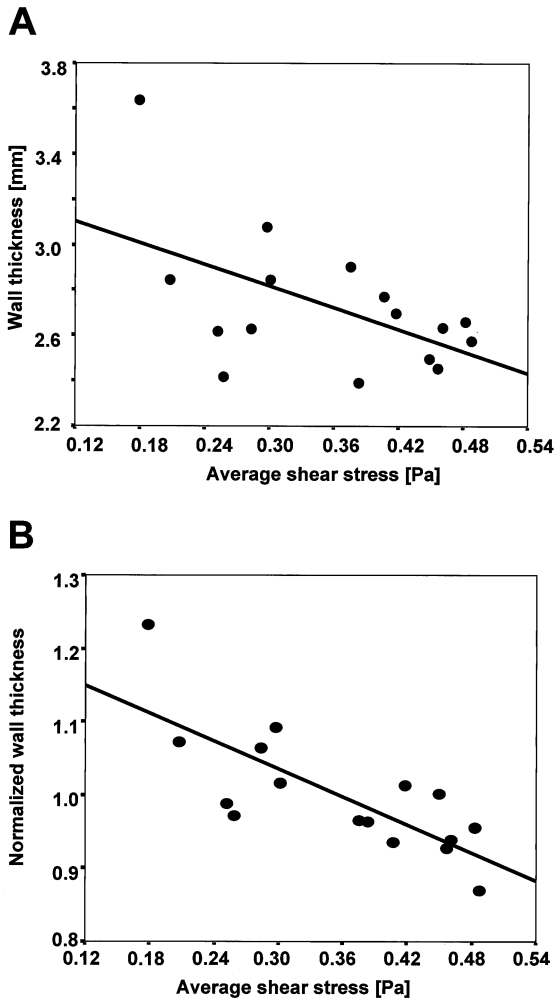

Figure 6. **(A)** Relationship between baseline wall thickness and shear stress (wall $\text{thickness}_{\text{baseline}} = -1.6 \times \text{SS} + 3.3$ [mm], $r^2 = 0.29$, $p < 0.05$). **(B)** Relationship between normalized wall thickness and shear stress (normalized wall thickness $= -0.63 \times \text{SS} + 1.23$, $r^2 = 0.59$, $p < 0.05$).

the cardiac cycle, which ranged from -0.05 to 0.79 N/m^2, result from inaccuracies in the method of the SS determination. Besides, the average SS values during the cardiac cycle were in the same range as determined by Suzuki et al. (26), who applied phase-contrast MRI in healthy young volunteers. They showed average shear rates of 97 ± 29 s^{-1} and 170 ± 43 s^{-1} at the inner and outer curve of the descending aorta respectively, implying a SS range of approximately 0.3 to 0.5 Pa. Interestingly, SS measurements in the abdominal aorta derived from phase-contrast MRI (4,11,27) appeared to deliver similar average SS values over the course of the cardiac cycle (0.18 to 0.95 N/m^2), as measured in the thoracic aorta.

Relationship between WT and SS. The SS determined in healthy young volunteers was used to study whether the SS governs the location where, in the presence of atherosclerotic risk factors, plaques start to develop and will be observed in the older, asymptomatic patients. Because severe plaques could protrude into the lumen, altering the local SS distribution, the SS distribution in healthy young subjects represents the natural SS distribution, permitting the study of history-related plaque generation and progression.

The observed rotational movement of the low SS regions from proximal to distal (Fig. 5) in the thoracic aorta is in agreement with previous observations of helical patterns in blood velocity in the descending thoracic aorta (7,29). Atherosclerotic WT was observed at the low SS regions (Fig. 6), explaining the helical pattern in the atherosclerotic wall thickening (Fig. 3). Similar helical patterns were observed in the sites of increased permeability for macromolecules in the thoracic aorta (30) and in monocyte deposition in the abdominal aorta (31), both of which are precursors of lesions formation.

The normalization of the WT showed that the thickest plaque in a segment is always located at the low SS locations regardless of the absolute thickness. This analysis emphasizes that atherosclerotic plaque buildup starts and progresses at low SS regions, confirming earlier studies on the relationship between atherosclerotic plaque and SS in coronary arteries (3,32,33), carotid arteries (5), and the abdominal aorta (4). Because several studies have shown that SS is regulated by the endothelium, which is mediated by nitric oxide production, plaque buildup is compensated for by positive vascular remodeling, preventing the aorta from narrowing, and maintaining high SS conditions (32).

Plaque regression. The benefits associated with hypolipidemic interventions have been clearly established by several large clinical trials both at primary and secondary prevention levels. In our patient group, who were not previously exposed to statins and who were newly diagnosed as hypercholesteremic, a reduction in 35% of LDL during a period of two years attributed to plaque regression as described previously. These results are confirmed by data of Jensen et al. (34) and Lima et al. (35), who showed plaque regression after 12 months with a 42% LDL reduction and 6 months with a 25% LDL reduction, respectively, because of simvastatin.

Despite the clinical outcomes, the mechanisms of action of the observed benefits are not well established. The stabilization of lipid-rich (vulnerable) plaques, due to lipid removal from the lesions, is considered the most widely accepted (10,36). Our data showed that the extent of plaque regression is related to the baseline thickness (Fig. 4) but is not mediated by SS. Because MR cross sections containing quadrants with plaques and with no intimal thickening were analyzed, and taking a plaque progression of approximately 10% yearly into account (37), this result can most likely not be attributed to the statistically driven regression to the mean. Our data allow the speculation that the lipid removal for the plaque (lipid efflux) may not occur through the luminal side but via transport from the vasa vasorum. Indeed, the thick fibrotic cap seems to serve as a barrier for cholesterol efflux. Recent reports highlight the role of adventitial vascularization in atherosclerosis and may support the concept of lipid

efflux via the vasa vasorum as an alternative mechanism for plaque regression and stabilization.

Study limitations. To estimate the influence of SS on plaque regression attributed to statin treatment in the asymptomatic hypercholesterolemic patients, we used the SS determined from the healthy volunteers. Because these patients were asymptomatic and only occasionally showed plaque protruding into the lumen, we argued that the SS *distribution* would not yet have been influenced by the disease. Of course, it is reported that in patients having atherosclerotic disease, the spiral flow velocity distribution in the *aortic arch* might be reduced (8,38) but, as stated previously, lower velocities would only minimally influence the relative SS distribution. Because we aimed at studying differences in plaque regression attributed to the relative SS distribution, the absolute SS values are of less importance.

A black-blood MRI sequence, which carried the potential of artifacts attributed to low flow, was used to determine the local WT in the thoracic aorta. Obviously, it might have confounded the WT-SS relationship. Because the lowest-average SS measured was 0.18 Pa, resulting from velocities of approximately 6 cm/s at 1 mm distance of the wall (and thus 3 cm/s at 0.5 mm from the wall), and accounting for the MRI taking a few minutes, it seems unlikely that this would have potentially influenced the WT data and thus the WT-SS relationship.

For the SS calculations, only the axial velocity component was used. It cannot be ignored that this approach underestimates the total shear rate. However, the underestimation would be approximately 5% at a maximum because the nonaxial shear components, which are approximately 25% of the axial shear component, are only minimally reflected in the total vector summation of the shear rates (26). Therefore, omitting the nonaxial components would hardly influence the overall SS distribution. Moreover, the acquisition of the small nonaxial velocity components could easily introduce errors.

Conclusions. Magnetic resonance imaging has surfaced as one of the most promising imaging methodologies for the noninvasive identification of atherosclerotic plaques and determination of local SS data. Our data, which show a correlation between WT and average low SS locations, support the role of local hemodynamics in the development and progression of aortic atherosclerotic lesions. Furthermore, local SS does not seem to be the major modulator for plaque regression by lipid-lowering interventions. Therefore, our data seem to suggest that other mechanisms are involved in the lipid-reversal mechanism.

Reprint requests and correspondence: Dr. Juan J. Badimon, Professor of Medicine, Cardiovascular Biology Research Laboratory, Mount Sinai School of Medicine, One Gustave L. Levy Place, Box 1030, New York, New York 10029-6574. E-mail: juan.badimon@mssm.edu.

REFERENCES

1. Sabbah HN, Khaja F, Brymer JF, Hawkins ET, Stein PD. Blood velocity in the right coronary artery: relation to the distribution of atherosclerotic lesions. Am J Cardiol 1984;53:1008–12.
2. Friedman MH, Brinkman AM, Qin JJ, Seed WA. Relation between coronary artery geometry and the distribution of early sudanophilic lesions. Atherosclerosis 1993;98:193–9.
3. Krams R, Wentzel J, Oomen J, et al. Evaluation of endothelial shear stress and 3D geometry as factors determining the development of atherosclerosis and remodeling in human coronary arteries in vivo. Combining 3D reconstruction from angiography and IVUS (ANGUS) with computational fluid dynamics. Arterioscler Thromb Vasc Biol 1997;17:2061–5.
4. Moore JE Jr., Xu C, Glagov S, Zarins CK, Ku DN. Fluid wall shear stress measurements in a model of the human abdominal aorta: oscillatory behavior and relationship to atherosclerosis. Atherosclerosis 1994;110:225–40.
5. Masawa N, Glagov S, Zarins CK. Quantitative morphologic study of intimal thickening at the human carotid bifurcation: I. Axial and circumferential distribution of maximum intimal thickening in asymptomatic, uncomplicated plaques. Atherosclerosis 1994;107:137–46.
6. Yamamoto T, Ogasawara Y, Kimura A, et al. Blood velocity profiles in the human renal artery by Doppler ultrasound and their relationship to atherosclerosis. Arterioscler Thromb Vasc Biol 1996;16:172–7.
7. Kilner PJ, Yang GZ, Mohiaddin RH, Firmin DN, Longmore DB. Helical and retrograde secondary flow patterns in the aortic arch studied by three-directional magnetic resonance velocity mapping. Circulation 1993;88:2235–47.
8. Houston JG, Gandy SJ, Sheppard DG, Dick JB, Belch JJ, Stonebridge PA. Two-dimensional flow quantitative MRI of aortic arch blood flow patterns: effect of age, sex, and presence of carotid atheromatous disease on prevalence of spiral blood flow. J Magn Reson Imaging 2003;18:169–74.
9. Corti R, Fayad ZA, Fuster V, et al. Effects of lipid-lowering by simvastatin on human atherosclerotic lesions: a longitudinal study by high-resolution, noninvasive magnetic resonance imaging. Circulation 2001;104:249–52.
10. Zhao XQ, Yuan C, Hatsukami TS, et al. Effects of prolonged intensive lipid-lowering therapy on the characteristics of carotid atherosclerotic plaques in vivo by MRI: a case-control study. Arterioscler Thromb Vasc Biol 2001;21:1623–9.
11. Pedersen EM, Oyre S, Agerbaek M, et al. Distribution of early atherosclerotic lesions in the human abdominal aorta correlates with wall shear stresses measured in vivo. Eur J Vasc Endovasc Surg 1999;18:328–33.
12. Corti R, Fuster V, Fayad ZA, et al. Lipid lowering by simvastatin induces regression of human atherosclerotic lesions: two years' follow-up by high-resolution noninvasive magnetic resonance imaging. Circulation 2002;106:2884–7.
13. Carr JC, Finn JP. MR imaging of the thoracic aorta. Magn Reson Imaging Clin N Am 2003;11:135–48.
14. Mintz GS, Nissen SE, Anderson WD, et al. American College of Cardiology clinical expert consensus document on standards for acquisition, measurement and reporting of intravascular ultrasound studies (IVUS). A report of the American College of Cardiology Task Force on Clinical Expert Consensus Documents. J Am Coll Cardiol 2001;37:1478–92.
15. Wentzel JJ, Krams R, Schuurbiers JC, et al. Relationship between neointimal thickness and shear stress after Wallstent implantation in human coronary arteries. Circulation 2001;103:1740–5.
16. Jaffer FA, O'Donnell CJ, Larson MG, et al. Age and sex distribution of subclinical aortic atherosclerosis: a magnetic resonance imaging examination of the Framingham Heart Study. Arterioscler Thromb Vasc Biol 2002;22:849–54.
17. Khoury Z, Gottlieb S, Stern S, Keren A. Frequency and distribution of atherosclerotic plaques in the thoracic aorta as determined by transesophageal echocardiography in patients with coronary artery disease. Am J Cardiol 1997;79:23–7.
18. Fazio GP, Redberg RF, Winslow T, Schiller NB. Transesophageal echocardiographically detected atherosclerotic aortic plaque is a marker for coronary artery disease. J Am Coll Cardiol 1993;21:144–50.

19. Amarenco P, Cohen A, Tzourio C, et al. Atherosclerotic disease of the aortic arch and the risk of ischemic stroke. N Engl J Med 1994;331: 1474–9.
20. Shunk KA, Garot J, Atalar E, Lima JA. Transesophageal magnetic resonance imaging of the aortic arch and descending thoracic aorta in patients with aortic atherosclerosis. J Am Coll Cardiol 2001;37: 2031–5.
21. Fayad ZA, Nahar T, Fallon JT, et al. In vivo magnetic resonance evaluation of atherosclerotic plaques in the human thoracic aorta: a comparison with transesophageal echocardiography. Circulation 2000; 101:2503–9.
22. Cohen A, Tzourio C, Bertrand B, Chauvel C, Bousser MG, Amarenco P. Aortic plaque morphology and vascular events: a follow-up study in patients with ischemic stroke. FAPS Investigators. French Study of Aortic Plaques in Stroke. Circulation 1997;96:3838–41.
23. Gore EA. Diseases of non-coronary arteries. In: Gould SE, editor. Pathology of the Heart and Blood Vessels. Springfield, IL: Charles & Thomas, 1968:953–60.
24. Strong JP, Malcom GT, McMahan CA, et al. Prevalence and extent of atherosclerosis in adolescents and young adults: implications for prevention from the Pathobiological Determinants of Atherosclerosis in Youth Study. JAMA 1999;281:727–35.
25. Bogren HG, Buonocore MH. 4D magnetic resonance velocity mapping of blood flow patterns in the aorta in young vs. elderly normal subjects. J Magn Reson Imaging 1999;10:861–9.
26. Suzuki J, Shimamoto R, Nishikawa J, et al. Vector analysis of the hemodynamics of atherogenesis in the human thoracic aorta using MR velocity mapping. Am J Roentgenol 1998;171:1285–90.
27. Oyre S, Ringgaard S, Kozerke S, et al. Accurate noninvasive quantitation of blood flow, cross-sectional lumen vessel area and wall shear stress by three-dimensional paraboloid modeling of magnetic resonance imaging velocity data. J Am Coll Cardiol 1998;32:128–34.
28. Cheng CP, Parker D, Taylor CA. Quantification of wall shear stress in large blood vessels using Lagrangian interpolation functions with cine phase-contrast magnetic resonance imaging. Ann Biomed Eng 2002;30:1020–32.
29. Frazin LJ, Lanza G, Vonesh M, et al. Functional chiral asymmetry in descending thoracic aorta. Circulation 1990;82:1985–94.
30. Barakat AI, Uhthoff PA, Colton CK. Topographical mapping of sites of enhanced HRP permeability in the normal rabbit aorta. J Biomech Eng 1992;114:283–92.
31. Buchanan JR, Kleinstreuer C, Hyun S, Truskey GA. Hemodynamics simulation and identification of susceptible sites of atherosclerotic lesion formation in a model abdominal aorta. J Biomech 2003;36: 1185–96.
32. Wentzel JJ, Janssen E, Vos J, et al. Extension of increased atherosclerotic wall thickness into high shear stress regions is associated with loss of compensatory remodeling. Circulation 2003;108:17–23.
33. Stone PH, Coskun AU, Kinlay S, et al. Effect of endothelial shear stress on the progression of coronary artery disease, vascular remodeling, and in-stent restenosis in humans: in vivo 6-month follow-up study. Circulation 2003;108:438–44.
34. Jensen LO, Thayssen P, Pedersen KE, Stender S, Haghfelt T. Regression of coronary atherosclerosis by simvastatin: a serial intravascular ultrasound study. Circulation 2004;110:265–70.
35. Lima JA, Desai MY, Steen H, Warren WP, Gautam S, Lai S. Statin-induced cholesterol lowering and plaque regression after 6 months of magnetic resonance imaging-monitored therapy. Circulation 2004;110:2336–41.
36. Crisby M, Nordin-Fredriksson G, Shah PK, Yano J, Zhu J, Nilsson J. Pravastatin treatment increases collagen content and decreases lipid content, inflammation, metalloproteinases, and cell death in human carotid plaques: implications for plaque stabilization. Circulation 2001;103:926–33.
37. Von Birgelen C, Hartmann M, Mintz GS, et al. Spectrum of remodeling behavior observed with serial long-term (≥12 months) follow-up intravascular ultrasound studies in left main coronary arteries. Am J Cardiol 2004;93:1107–13.
38. Bogren HG, Buonocore MH, Valente RJ. Four-dimensional magnetic resonance velocity mapping of blood flow patterns in the aorta in patients with atherosclerotic coronary artery disease compared to age-matched normal subjects. J Magn Reson Imaging 2004;19:417–27.